Identifying parameters controlling soil delayed behaviour from laboratory and in situ pressuremeter testing

Zhen-Yu Yin, Pierre-Yves Hicher

Identifying parameters controlling soil delayed behaviour from laboratory and *in situ* pressuremeter testing

Zhen-Yu Yin and Pierre-Yves Hicher

Research Institute in Civil and Mechanical Engineering, GeM UMR CNRS 6183, Ecole Centrale de Nantes, BP 92101, 44321 Nantes, France

The aim of this paper is to present a methodology for identifying the soil parameters controlling the delayed behaviour from laboratory and *in situ* pressuremeter tests by using an elasto-viscoplastic model (EVP-MCC) based on Perzyna's overstress theory and on the elasto-plastic Modified Cam Clay model. The influence of both the model parameters and the soil permeability was studied under the loading condition of pressuremeter tests by coupling the proposed model equations with Biot's consolidation theory. On the basis of the parametric study, a methodology for identifying model parameters and soil permeability by inverse analysis from three levels of constant strain rate pressuremeter tests was then proposed and applied on tests performed on natural Saint-Herblain clay. The methodology was validated by comparing the optimized values of soil parameters and the values of the same parameters obtained from laboratory test results, and also by using the identified parameters to simulate other tests on the same samples. The analysis of the drainage condition and the strain rate effect during a pressuremeter test demonstrated the coupled influence of consolidation and viscous effects on the test results. The numerical results also showed that the inverse analysis procedure could successfully determine the parameters controlling the time-dependent soil behaviour.

KEY WORDS: viscoplasticity; consolidation; Modified Cam Clay; parameter identification; soft clay; pressuremeter test

1. INTRODUCTION

The identification of soil parameters from *in situ* tests, such as pressuremeter tests consisting in studying the expansion of a cylindrical cavity within the soil, has been commonly used since the

invention of the pressuremeter apparatus by Menard [1]. Zentar *et al.* [2] divided the methods used for this purpose into three categories: (a) those based on empirical or semi-empirical relationships between soil properties and pressuremeter parameters; (b) those based on the theoretical development of cylindrical cavity expansion solutions; and (c) those based on numerical simulations of the test. It is noted that the proper calibration of soil parameters depends on the number of parameters to be optimized for a selected model and the number of observations, as shown by Zentar *et al.* [2] during the optimization procedure and as indicated by Calvello and Finno [3].

In the past few decades, several studies for identifying soil parameters from pressuremeter tests have been found in the literature, i.e. Anderson *et al.* [4], Bahar *et al.* [5], Pye [6], Hicher and Michali [7], Zentar *et al.* [2], Rangeard *et al.* [8], etc. However, few of these are concerned by the delayed behaviour of fine soils. However, the strain-rate dependency of soft soils has a significant influence on the selection of design parameters. A constitutive model taking into account the time-dependent behaviour should be recommended, although additional parameters of viscosity for this kind of model would result in difficulties during the selection of the soil parameters by optimization procedure. In order to study this kind of problem, we based our analysis on experimental results obtained with the equipment called pressio-triax [2, 8], which could simulate a self-boring pressuremeter (SBP) with pore water pressure measurement at the cavity wall in tightly controlled laboratory conditions.

In the first part of this paper, we briefly present the development of an elasto-viscoplastic model with its implementation in a finite element program CESAR_LCPC. The motivation behind this initial work lied in the fact that we wished to have a viscoplastic version of the Modified Cam Clay model for which parameter identification procedures had already been developed [2, 8]. Then a back analysis method for identifying soil mechanical and hydraulic parameters from pressuremeter tests with three different strain rates is presented and applied on tests performed on natural Saint-Herblain clay. The methodology is validated by comparing the optimized values of soil parameters with the values of the same parameters obtained from laboratory test results, and also by using the identified parameters to simulate other tests on the same samples. The drainage condition during a pressuremeter test as a function of the strain rate and the permeability as well as the strain rate effect on the pressuremeter curve is analysed. Finally, an application to *in situ* pressuremeter tests is carried out.

2. ELASTO-VISCOPLASTIC CONSTITUTIVE MODEL

An elasto-viscoplastic model, named EVP-MCC, based on the framework of Perzyna's overstress theory and Modified Cam Clay elasto-plastic model was developed by Yin *et al.* [9]. The proposed model has two additional viscosity parameters besides the parameters of the Cam clay model and is an attempt to provide a simple but realistic enough approach in modelling time-dependent behaviour of clayey soils subjected to monotonic proportional loading paths. Some limitations of this model are discussed in the following sections.

According to the assumption of Perzyna's overstress theory [10, 11], the viscous effects are negligible in the elastic region. In other words, the elastic strains are time independent, whereas the inelastic strains are time dependent. We define a static yield criterion f_s, which represents a reference yield surface for the material, corresponding to the elastic limit with null viscoplastic flow rate. Its initial shape depends on the consolidation pressure p_c^s. The expansion of the static yield surface, which represents the hardening of the material, is expressed by the variation in the

consolidation pressure due to the inelastic volumetric strain ε_v^{vp}:

$$\mathrm{d}p_c^s = p_c^s \cdot \frac{1+e_0}{\lambda-\kappa} \cdot \mathrm{d}\varepsilon_v^{vp} = \frac{p_c^s}{\beta^*} \cdot \mathrm{d}\varepsilon_v^{vp} \tag{1}$$

where p_c^s is the static consolidation pressure, ε_v^{vp} the inelastic volumetric strain, and β^* the compressibility index.

A dynamic loading yield criterion f_d is defined to represent the current state of stress and is expressed as follows:

$$f_d = \frac{q^2}{M^2} + p' \cdot (p' - p_c^d) = 0 \tag{2}$$

where p_c^d is the dynamic consolidation pressure, M the slope of the critical state line, p' representing the effective mean stress $p' = (\sigma'_{11} + \sigma'_{22} + \sigma'_{33})/3$, and q the deviatoric stress, which is given by

$$q = \sqrt{3J_2} = \sqrt{[(\sigma'_{11} - \sigma'_{22})^2 + (\sigma'_{11} - \sigma'_{33})^2 + (\sigma'_{22} - \sigma'_{33})^2 + 6(\sigma'^2_{12} + \sigma'^2_{13} + \sigma'^2_{23})]/2}$$

We then define a distance F between the dynamic loading and the static yield surfaces at a given time t as $F = p_c^d / p_c^s$. Based on the distance F, the scaling function $\mu\Phi(F)$, which controls the amplitude of the viscoplastic strain rate, is taken as an exponential form as follows:

$$\mu \cdot \Phi(F) = \mu \cdot (\exp[N \cdot (F-1)] - 1) \tag{3}$$

where μ and N are the viscosity parameters of the model. As expressed in Equation (3), the model cannot describe the volumetric relaxation process, unless the initial state is not considered at equilibrium. The flow rule for the viscoplastic strain rate, in a simple case of infinitesimal strain field, follows the form proposed by Perzyna [11]:

$$\dot{\varepsilon}_{ij}^{vp} = \mu \langle \phi(F) \rangle \frac{\partial f_d}{\partial \sigma'_{ij}} \tag{4}$$

where the function of MacCauley is

$$\langle F \rangle = \begin{cases} 0 & \text{for } F \leqslant 0 \\ F & \text{for } F > 0 \end{cases}$$

The principles of the elasto-viscoplastic model EVP-MCC are illustrated by the effective stress path of an undrained triaxial test presented in Figure 1. The stress state '*A*' represents an initially normally K_0' consolidation state. Along the loading stress path '*A*–*B*–*C*', viscoplastic volumetric strains occur during loading and cause the static yield surface to expand in the stress space. As point *C* approaches *C′*, corresponding to the critical state, the soil is subjected to a constant amount of overstress, which provokes an increase in the deviatoric strain at constant strain rate, without any volumetric strain.

As for the creep stress path '*B*–*D*', the static yield surface expands with the time-dependent plastic volumetric strain as a function of the amount of overstress. If the static yield surface can reach the actual stress point, the equilibrium is obtained and the strain will be stabilized with time. If not, the effective stress will continue to evolve until it reaches the critical state at point *D′* where

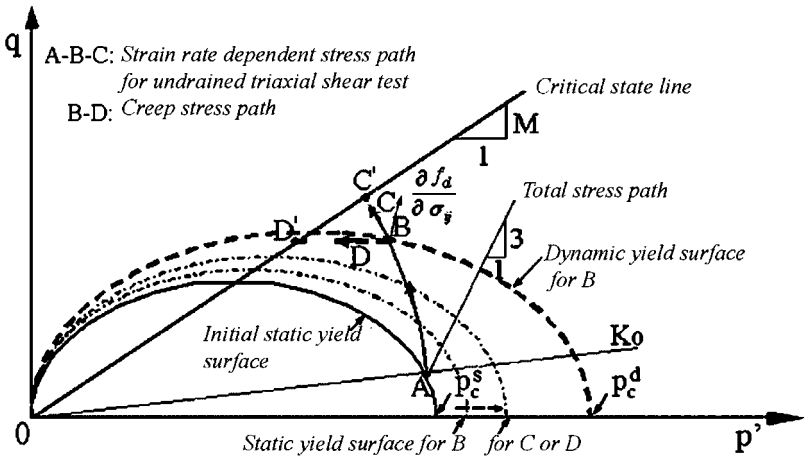

Figure 1. Schematic behaviour of the EVP-MCC model during CAU triaxial compression and triaxial creep tests.

it will stop because no plastic volumetric strain will develop, but deviatoric strain will continue to increase.

Taking into account the elastic stress–strain relationships, the constitutive equations of the viscoplastic model for normally consolidated clays are derived as follows:

$$\dot{\varepsilon}_{ij} = \frac{\dot{s}'_{ij}}{2G} + \frac{\dot{p}'}{3K}\delta_{ij} + \mu\langle\phi(F)\rangle\left(\frac{3s'_{ij}}{M^2} + (2p' - p_c^{\mathrm{d}})\frac{\delta_{ij}}{3}\right) \tag{5}$$

where σ'_{ij} is the effective stress tensor and $\dot{\varepsilon}_{ij}^{\mathrm{vp}}$ the inelastic strain rate tensor.

The basic finite element scheme for the proposed model is similar to that presented by Oka *et al.* [12] and Hinchberger and Rowe [13]. For a coupled consolidation analysis based on Biot's theory, the relationship of the load increment is given by applying the principle of virtual work to the equilibrium equation as shown by Oka *et al.* [12]:

$$\begin{aligned}\int_V [\Delta\varepsilon]^{\mathrm{T}} \cdot [\Delta\sigma]\,\mathrm{d}V &= \int_V [\Delta\varepsilon]^{\mathrm{T}} \cdot [\Delta\sigma']\,\mathrm{d}V + \int_V [\Delta\varepsilon]^{\mathrm{T}} \cdot [\Delta u_w]\,\mathrm{d}V \\ &= \int_V [\Delta d]^{\mathrm{T}} \cdot [\Delta F_b]\,\mathrm{d}V + \int_S [\Delta d]^{\mathrm{T}} \cdot [\Delta T]\,\mathrm{d}S\end{aligned} \tag{6}$$

The equation of continuity for water flow can be expressed as follows:

$$\int_{\mathrm{vol}} [b]\left[\sum_{i=1}^{3} \frac{k_i}{\gamma_w}\frac{\partial^2 u_w}{\partial x_i^2} + \frac{\partial v}{\partial t}\right]\mathrm{d(vol)} = 0 \tag{7}$$

where k_i is the hydraulic conductivity in three coordinate directions, γ_w is the unit weight of the pore water, and v is the seepage velocity.

The coupled finite element equations were well documented by several researchers (e.g. [12–14]).

3. IDENTIFICATION OF SOIL PARAMETERS FROM PRESSUREMETER TESTS

3.1. Methodology of parameter identification by inverse analysis

The mechanical problem is traditionally resolved by calculating the response (R) of a mechanical system (S) including the constitutive model (M) and its parameters (P) subjected to the actions (A). It corresponds to what is called the direct problems (Figure 2(a)) and is expressed in mathematical terms as follows:

$$R = F(S) \tag{8}$$

However, in inverse analysis (Figure 2(b)), the parameters (P) of the given model (M) should be calibrated by using an optimization procedure that consists of iteratively changing the input values of the parameters until the calculated results match the observed data, i.e. laboratory or *in situ* tests results. The methodology of the inverse analysis is shown in Figure 3. During the optimization procedure, the difference between observation data and model prediction is expressed as follows:

$$L_n(P) = \frac{1}{t_1 - t_0} \int \| R^*(t) - R(S,t) \| \, \mathrm{d}t \tag{9}$$

where the notation $\| \ldots \|$ represents a norm in the space variable, $t_1 - t_0$ is the time of observation, and $R^*(t) - R(S,t)$ is the difference between experimental and numerical data. Owing to the measurements at discrete moments, the integral of $L_n(P)$ can be replaced by a sum and the length of observation by the number of measurements. The difference between measured and predicted data is then expressed as follows:

$$L_n(P) = \frac{1}{M_n} \sum_{i}^{M_n} (R_i^* - R_i)^2 \tag{10}$$

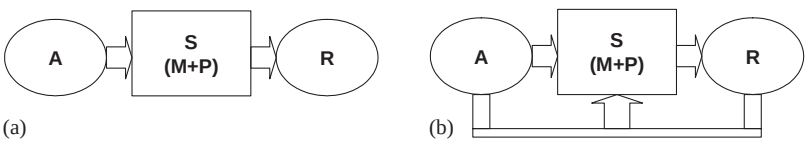

Figure 2. Resolution of the (a) direct problem and (b) inverse problem.

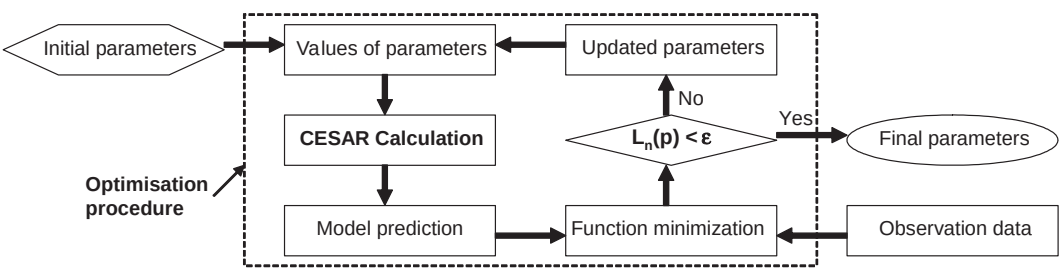

Figure 3. Procedure of parameter identification by inverse analysis.

$L_n(P) < \varepsilon$ (ε is a given tolerance) can be used as a discriminate function to judge the convergence of the iterative process.

3.2. Experimental results

The pressuremeter tests were conducted by using a special pressuremeter apparatus called pressio-triax, which allows reproducing the pressuremeter test conditions in a triaxial cell. As described by Zentar *et al.* [2] and Rangeard *et al.* [8], the pressio-triax was developed in order to study the pressuremeter loading in tightly controlled laboratory conditions. A special aspect of this equipment is its ability to measure the pore water pressure evolution at the cavity wall during testing. On the basis of the test results obtained with this apparatus, Rangeard *et al.* [8] have developed a methodology for identifying mechanical and hydraulic parameters of clayey materials, using an elastoplastic model, the Modified Cam Clay model. In this study, we extended this methodology in order to take into account the determination of the viscosity parameters of the EVP-MCC. The tests were performed on Saint-Herblain clay, a river clayey alluvial deposit from the Loire Paleolithic period, characterized by a high plasticity index ($I_p = 42$) and slightly or moderately organic. The consolidation stress state was defined by $\sigma_1 = 85\,\text{kPa}$, $\sigma_2 = \sigma_3 = 68\,\text{kPa}$, $u = 56.5\,\text{kPa}$ for samples taken at a depth of 5.5–6.5 m, and $\sigma_1 = 110\,\text{kPa}$, $\sigma_2 = \sigma_3 = 90\,\text{kPa}$, $u = 68\,\text{kPa}$ for samples at a depth of 6.5–7.5 m. The physical and mechanical characteristics for each test are summarized in Table I, which includes the strain rate values of the performed pressio-triax tests.

An oedometer test at a constant strain rate of $3.3 \times 10^{-6}\,\text{s}^{-1}$ was carried out on a sample of the Saint-Herblain clay at a depth of 6.9–6.95 m using a modified oedometer apparatus [15]. Lateral stress could also be measured during the test. The parameters deduced from the one-dimensional consolidation curves are presented in Table II. The soil is slightly overconsolidated and $K_0' = 0.55$.

Table I. Physical and mechanical characteristics of Saint-Herblain clay samples.

Specimen	Depth (m)	w (%)	e_i	γ (kN/m^3)	Strain rate (s^{-1})
Pre1A (CR)	6.5–7.5	113	2.69	14.91	3×10^{-5}
Pre3A (SR)	5.5–6.5	97	2.23	13.96	3×10^{-5}
Pre3B (SR)	5.5–6.5	96	2.48	14.21	6×10^{-7}
Pre3D (SR)	5.5–6.5	85	2.16	14.22	1.5×10^{-4}
Pre3F (SR)	5.5–6.5	90	2.51	14.41	6×10^{-6}
Pre3H (RE)	5.5–6.5	93	2.29	14.35	6×10^{-5}
Tri1B (SR)	5.5–6.5	89	2.32	14.76	$2.8 \times 10^{-5\text{ to }-7}$
Tri1F (CR)	5.5–6.5	86	2.84	14.87	—
Oed1	6.5–7.5	87	2.26	14.85	3.3×10^{-4}, 6.6×10^{-5}
Oed2	5.5–6.5	93	2.61	14.88	—

CR, creep test; SR, strain rate test; and RE, relaxation test.

Table II. Parameters deduced from oedometer test.

Depth (m)	w (%)	e_i	γ (KN/m^3)	λ	κ	e_0	$\sigma'_{\text{ra},0}$ (kPa)	$\sigma'_{\text{v},0}$ (kPa)
6.9–6.95	87	2.26	14.85	0.43	0.02	2.1	29	52

$\sigma'_{\text{ra},0}$, radial preconsolidation pressure and $\sigma'_{\text{v},0}$, vertical preconsolidation pressure.

3.3. Numerical modeling of pressuremeter test

Numerical modelling of pressuremeter tests was performed by using the proposed elasto-viscoplastic model coupling the Biot consolidation theory in order to predict the stress evolution as well as the pore pressure change caused by the expansion of the cavity wall. During this expansion test, the soil was considered saturated and the permeability was kept constant. The initial stress state was taken to be equal to the *in situ* state described in the previous section.

The real geometry of the specimen was taken into account by considering a plane strain condition in the vertical direction and an axisymmetric condition in the horizontal direction with $a = 6.5\,\text{mm}$, $b = 35\,\text{mm}$, as shown in Figure 4. The value of the height H was taken to be equal to 6.5 mm. The mesh was composed of 27 elements with 138 nodes. The elements for all tests were isoparametric with eight integration points. The proposed elements and the mesh were verified dense enough to achieve accurate numerical solutions.

As for the boundary conditions, vertical displacement was prevented, whereas horizontal displacements could develop freely. The displacement was applied in the mini-pressuremeter probe on the side AD, and the cell pressure was maintained constant on the side BC. No water flow (flux $\phi = 0$) was allowed to pass through the four faces for the undrained boundary conditions.

3.4. Sensitivity to model parameters

The influence of the model parameters on the pressuremeter curve and the evolution of the pore pressure at cavity wall were examined by simulating a pressuremeter test at a strain rate of $6 \times 10^{-5}\,\text{s}^{-1}$ with an initial total stress $\sigma_1 = 85\,\text{kPa}$, $\sigma_2 = \sigma_3 = 68\,\text{kPa}$ and initial pore pressure $u_0 = 56.5\,\text{kPa}$. The reference values of the parameters for this test are given in Table III.

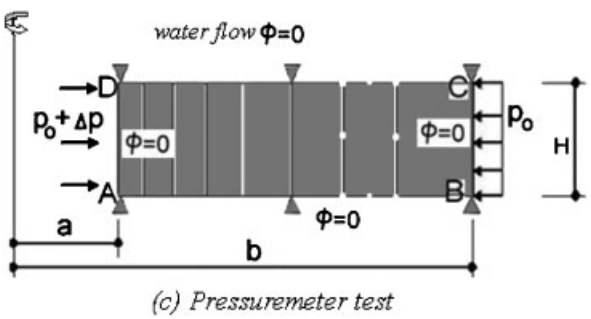

Figure 4. Finite element geometry for pressuremeter tests.

Table III. Reference values of EVP-MCC model and hydraulic parameters for natural Saint-Herblain clay.

E (kPa)	υ	β^*	M	p'_{c0} (kPa)	N	μ ($\text{s}^{-1}\,\text{kPa}^{-1}$)	k (m/s)
3500	0.3	0.16	1.25	30	10	1×10^{-9}	1×10^{-11}

The influence of the parameters common to the MCC and the EVP-MCC models $\{E, \upsilon, \beta^*, M, p'_{c0}\}$ is in accordance with the results presented by Zentar *et al.* [2] and Rangeard *et al.* [8]:

- the parameters E, M, p'_{c0} have a significant effect on the stress–strain relationship as well as on the evolution of pore pressure;
- the parameters υ and β^* have a very small effect on the evolution of the total stress and the pore pressure;
- only Young's Modulus E can change the initial slope of the strain–stress curve.

Special attention was paid to the influence of the viscosity parameters (N, μ). Their effects on the radial total stress and the pore pressure at the cavity wall are presented in Figure 5. Their evolutions are plotted as a function of the relative displacement at the cavity wall δ_{ra} = ratio of the cavity wall displacement to the initial cavity radius. We can note that N and μ have an important effect on the computed stress, especially for $5<N<20$ and $\mu<1\times10^{-6}$, and a small effect on the pore pressure. The information can be used to determine these two parameters from the sole total stress curve. To obtain the same stress evolution for a given constant strain rate, N and $\log(\mu)$ are

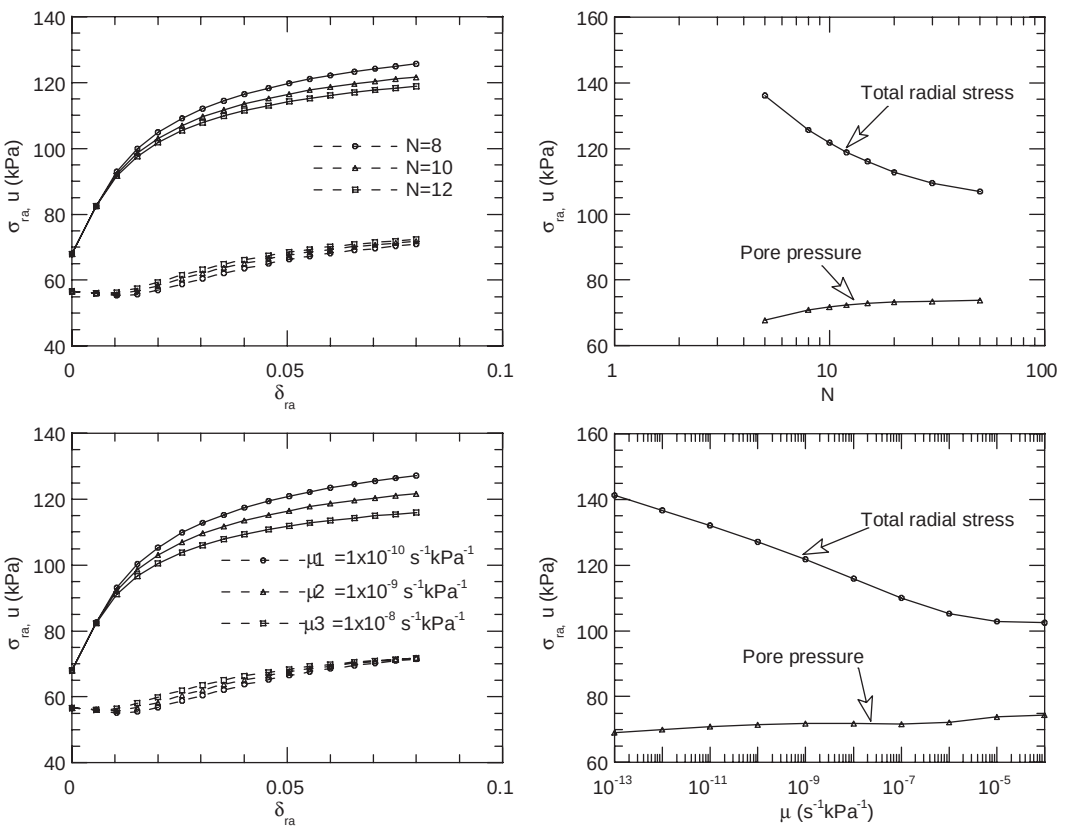

Figure 5. Effect of viscosity parameters on the total radial stress and the pore pressure for pressuremeter test.

related by a linear relationship as shown in Figure 6(a). For other strain rates, the selected values of (N, μ) produce much more changes on the stress–strain curve, as presented in Figure 6(b), where σ_{ra}^{*} represents the computed total radial stress for different values of the viscosity parameters normalized by the stress corresponding to ($N = 10$, $\mu = 1 \times 10^{-4}$). From this information, the values of (N, μ) can be determined from pressuremeter tests at three different strain rates.

The influence of (N, μ) on a strain holding stage (stress relaxation test) at a strain of 8% and on a stress holding stage (creep test) at a stress increment of 41 kPa after an initial constant strain rate loading was also studied and is presented in Figure 7. The results show the influence of (N, μ) on the evolution of the radial stress during a strain holding stage or on the radial strain during a creep test. It is therefore possible to determine the values of (N, μ) from either a relaxation test or a creep test.

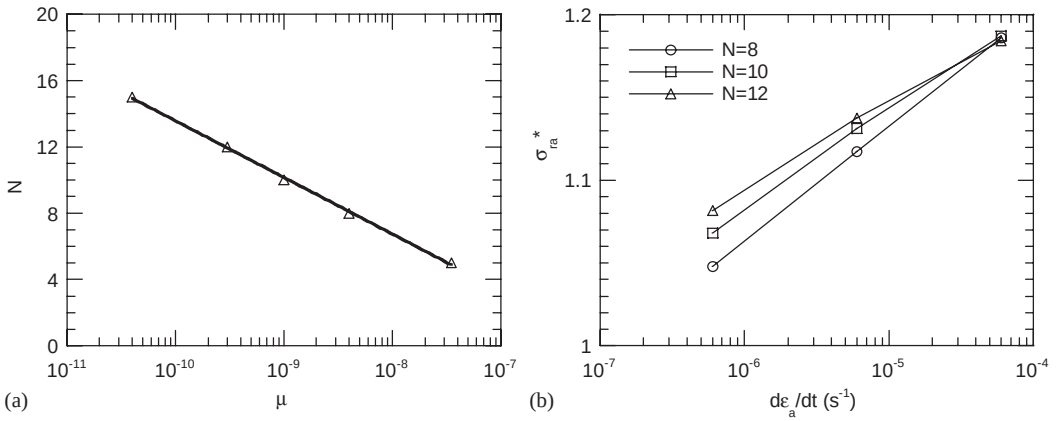

Figure 6. Coupling effect of viscosity parameters on the total radial stress for pressuremeter test.

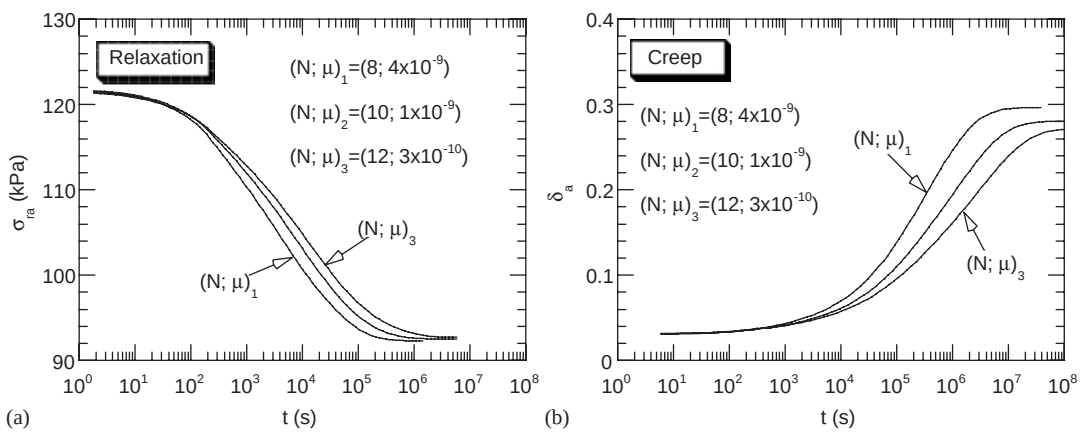

Figure 7. (a) A comparison of stress relaxation for different (N, μ) during strain holding stage and (b) a comparison of strain evolution for different (N, μ) during stress holding stage.

The soil permeability k has to be taken into account in pressuremeter tests. For tests in perfectly drained or undrained conditions, k has no influence on the stress and pore pressure responses, whereas for tests in partially drained condition, k has a significant effect. Figure 8 shows that the permeability has a significant effect on the pore pressure evolution for values between 10^{-8} and 10^{-12} m/s, and a very small effect for other values, which correspond to either perfectly drained or undrained conditions during the pressuremeter test. However, the permeability has a very small effect on the radial stress. We can point out that the influence of the viscosity parameters and of the soil permeability on the stress–strain relationship and on the pore pressure evolution is independent of each other. This information can be used to determine the soil permeability from the sole evolution of the pore pressure at cavity wall for given values of EVP-MCC parameters.

3.5. Identification procedure

Based on the previous parametric study, we firstly determined several parameters as follows:

- Poisson's ratio was taken to be equal to 0.3, which is a common value for clay.
- Young's modulus, which controls the initial slope of the radial stress–radial strain curves in the elastic region, was determined as $E = 3500$ kPa.
- The compressibility index was determined from oedometer tests: $\beta^* = (\lambda - \kappa)/(1+e_0) = (0.43-0.02)/(1+2.1) = 0.13$.

The procedure of parameter identification by inverse analysis, as presented in Figure 3, was employed to determine the other parameters from pressio-triax tests with three different strain rates. The iterative process to update the parameters takes the following order: $M \rightarrow p'_{c0} \rightarrow N \rightarrow m$ and k, as presented in Figure 9. The optimization loops (Table IV) were carried out as follows:

1. At first, an interval of acceptable values for the set of parameters $\{M, p'_{c0}, N, \mu, k\}$ was selected, such as in the first two lines in Table IV. The initial value of each parameter was then given as the average of the upper and lower bound values.

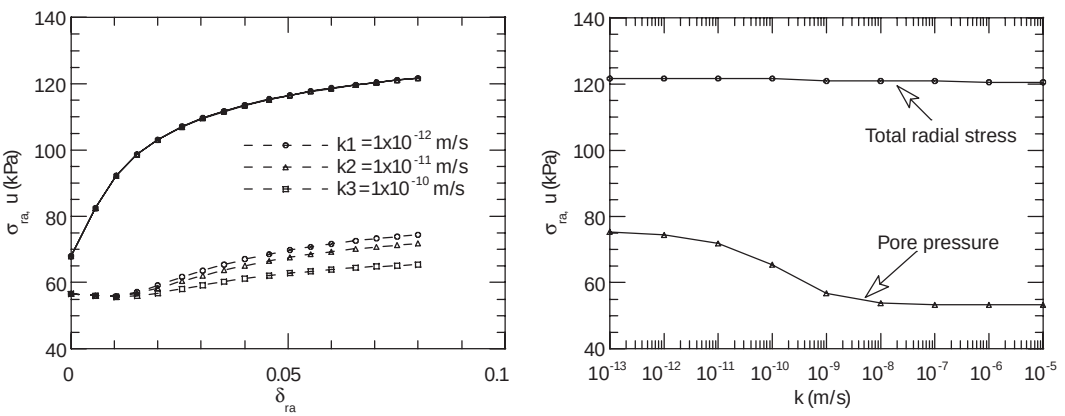

Figure 8. Permeability effects on radial stress and pore pressure responses for pressuremeter tests.

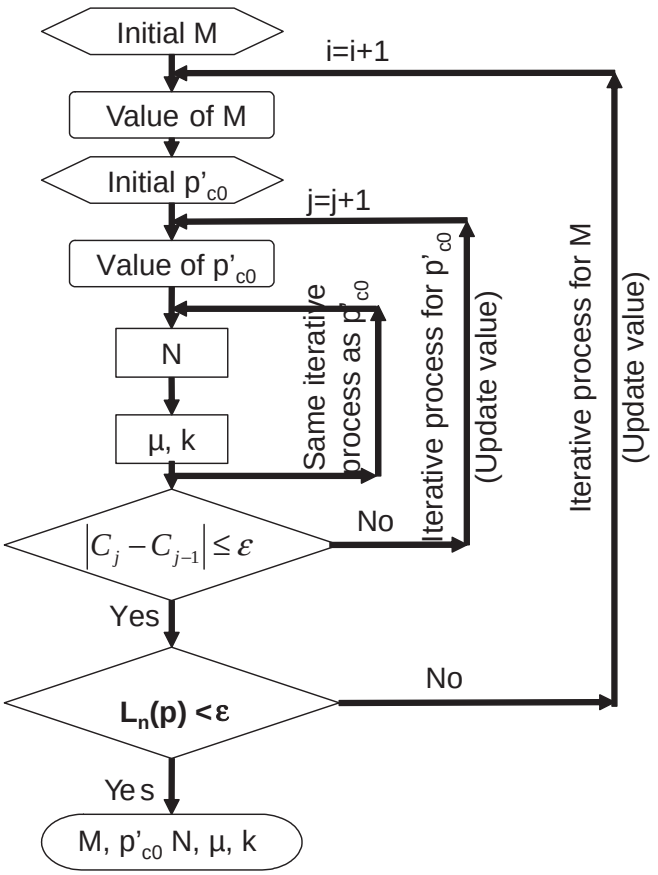

Figure 9. Iterative process to identify soil parameters in the order of $M \rightarrow p'_{c0} \rightarrow N \rightarrow m$ and k.

2. The incremental loop for determining M was carried out by using, at each step, the average value of the defined interval. For each value of M, the incremental loop for the determination of p'_{c0} was carried out by using the average value of the selected interval as for M. The interval of parameter values was re-defined by the updated parameters. In Table IV, 'UP' and 'LOW' mean selected parameter values defined as new upper and lower bounds, respectively, which result in predicted curves above and under, respectively, the experimental ones.
3. For each value of M and p'_{c0}, the values of N, μ, and k could be determined by using the same process as for p'_{c0}, and also with the re-definition of their bound values by the updated parameters. Noting the small influence of the viscosity parameters on the evolution of the pore pressure and the small effect of the permeability on the total stress evolution, the iterative process for the parameters μ and k was set in the same iterative loop.
4. The values of the parameters were assessed after the convergence of the calculation according to a criterion on the difference between the current step and the last step smaller than a given tolerance, as presented in Table IV for the iterating process concerning p'_{c0}, N, μ, and k with $M = 1$.

Table IV. Optimization loops for identifying soil parameters by inverse analysis.

Loop of M		Loop of p'_{c0}		Loop of N		Loop of μ, k			
M		p'_{c0} (kPa)		N		Log(μ)(s^{-1} kPa^{-1})		Log(k) (m/s)	
0.5	Low	25	Low	15	Low	−6	Low	−7	Low
1.5	Up	50	Up	5	Up	−15	Up	−15	Up
						−10.5	Up	−11	Low
						−8.25	Low	−13	Low
		37.5		10		−9.375	Low	−14	Low
						−9.938	Up	−14.5	Low
						−9.656	Up	−14.75	Low
		37.5	Low	10	Converge	−9.516	Converge	−14.875	Converge
1						−10.5	Up	−11	Low
						−8.25	Low	−13	Low
						−9.375	Up	−14	Low
				10		−8.813	Low	−14.5	Low
						−9.094	Up	−14.75	Low
						−8.953	Low	−14.875	Low
						−9.023	Low	−14.938	Low
		43.75		10	Low	−9.059	Converge	−14.969	Converge
						−10.5	Up	−11	Low
						−8.25	Up	−14	Low
				7.5		−7.125	Low	−14.5	Low
						−7.688	Low	−14.75	Low
						−7.969	Up	−14.875	Low
						−7.828	Up	−14.938	Low
		43.75	Up	7.5	Converge	−7.758	Converge	−14.969	Converge
						−10.5	Up	−11	Low
						−8.25	Low	−14	Low
						−9.375	Up	−14.5	Low
		40.625		10		−8.813	Low	−14.75	Low
						−9.094	Up	−14.875	Low
						−8.953	Low	−14.938	Low
1	Low	40.625	Converge	10	Converge	−9.023	Converge	−14.969	Converge
		37.5	Up	7.5	(Final)	−7.828	(Final)	−10.75	(Final)
		31.25	Up	9.375	(Final)	−8.813	(Final)	−10.75	(Final)
1.25		28.125	Low	11.25	(Final)	−9.375	(Final)	−10.75	(Final)
		29.688	Low	10	(Final)	−9.094	(Final)	−10.75	(Final)
		30.469	Up	10	(Final)	−9.023	(Final)	−10.75	(Final)
1.25	Converge	30.078	Converge	10	(Final)	−8.988	(Final)	−10.75	(Final)

up, upper bound value; low, lower bound value; and final, after convergence.

5. For the iterating process concerning M, once the calculation converged, that is, the difference between experimental data and calculation results became sufficiently small and stable, according to a criterion that allowed us to calculate the overall error between experimental and numerical results, we then obtained the final values of the parameters. In Table IV, we give the final values of the parameters at the end of the iterative process.

Figure 10 shows the predicted results after the convergence for $p'_{c0} = 40.6$ with $M = 1.0$. A good performance is achieved for the total stress curves, but not for the pore pressure curves. The iterative

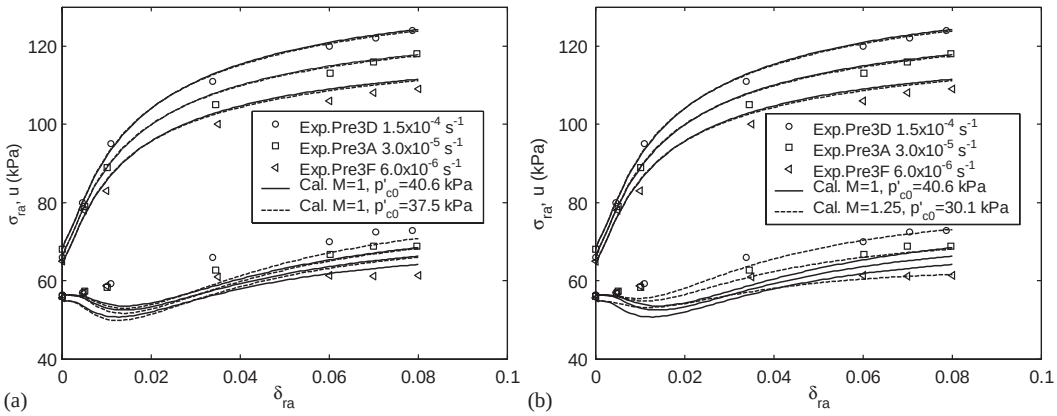

Figure 10. (a) Results for different p'_{c0} with $M=1.0$ and (b) results for different values of M.

Table V. Values of EVP-MCC model and hydraulic parameters of Saint-Herblain clay.

E (kPa)	υ	β^*	M	p'_{c0} (kPa)	N	μ ($s^{-1}\,kPa^{-1}$)	k (m/s)
3500	0.3	0.13	1.25	30.1	10	1.03×10^{-9}	1.78×10^{-11}

process goes to the next loop of M until a good general agreement is achieved, i.e. $L_n(P)<\varepsilon$. In Figure 10 one can see the numerical simulations obtained with the final set of parameters ($M=1.25$). The predicted results after the convergence of the whole iterative process are in good agreement with the whole set of experimental results. The final values of the parameters determined by the proposed procedure, in the last row of Table IV, are summarized in Table V.

4. VERIFICATION OF THE IDENTIFICATION PROCEDURE

The value of the slope of critical state line $M=1.25$ corresponds to a friction angle equal to 31°, which agrees well with the results of triaxial tests in compression performed on the same samples (Figure 11(a)) reported by Zentar [16]. The preconsolidation pressure $p'_{c0}=30.1$ kPa corresponds to an overconsolidated ratio OCR = 1.1 ($\sigma'_v=33.3$ kPa calculated at the depth of 6 m, $K'_0=0.55$ as measured by Zentar [16] and Rangeard [15]). Owing to the strain-rate-dependency of the soil strength, it appears reasonable that the optimized preconsolidation pressure was found smaller than the measured one ($p'_{c0}=37$–50 kPa by Rangeard *et al.* [8]). The value of the soil permeability $k=1.78\times10^{-11}$ m/s is smaller than the one measured from conventional oedometer tests (Figure 11(b)) by Yin [17]. It could be due to the fact that the permeability value was kept constant during the numerical simulation, not taking into account the change of void ratio during consolidation.

Furthermore, in order to examine the coherence of the set of parameters obtained by the identification procedure, a pressuremeter test at a constant strain rate of $6\times10^{-7}\,s^{-1}$ (Pre3B) and a constant strain rate test ($6\times10^{-5}\,s^{-1}$) with a relaxation stage (Pre3H) were simulated using the determined parameter values. The comparison between predicted and measured results, presented

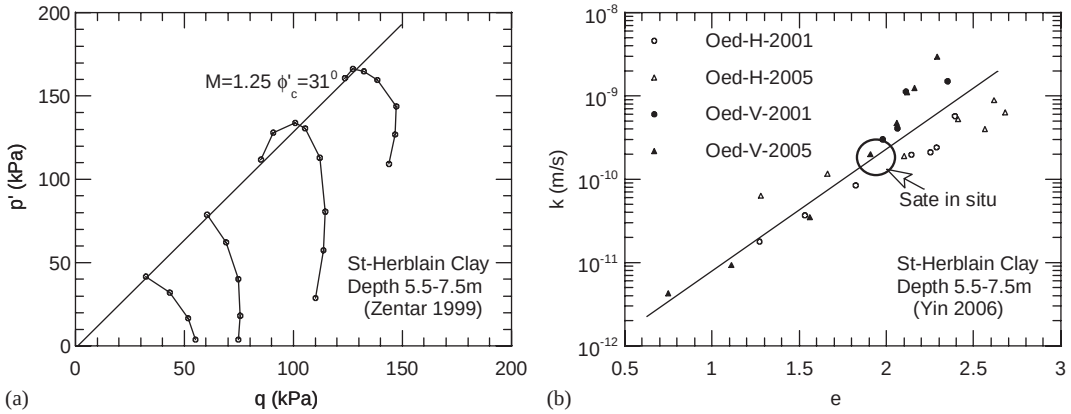

Figure 11. (a) Results in $q-p'$ space of the triaxial tests in compression and (b) soil permeability *versus* voids ratio by conventional oedometer tests (H, sample in the horizontal direction and V, sample in the vertical direction).

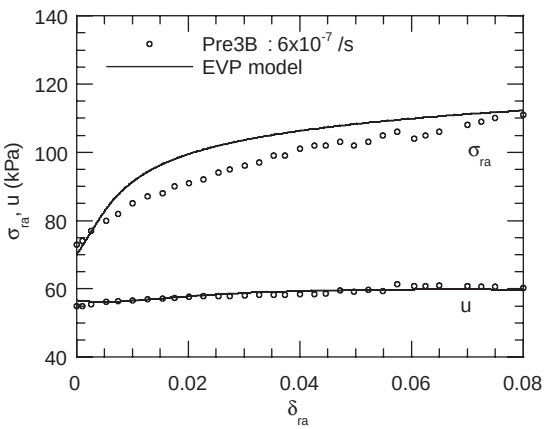

Figure 12. A comparison between experiment and simulation of strain rate tests.

in Figures 12 and 13, showed that the EVP-MCC is able to describe the time-dependent behaviour observed in pressuremeter tests and that the proposed method can be successfully applied for identifying the soil parameters. The time for dissipating the excess pore water pressure is identical for both numerical and experimental results during the relaxation stage, although the value of the predicted pore pressure is slightly smaller than the measured one.

Moreover, the determined set of parameters was taken for simulating a pressuremeter creep test (Pre1A), except for the value of the preconsolidation pressure $p'_{c0}=35\,\text{kPa}$ due to a different initial state of consolidation for a 1 m deeper sample. A good agreement between predicted and measured results was achieved, as presented in Figure 14. These different cases show the ability of the proposed procedure to identify correctly the soil parameters by means of pressuremeter tests with different strain rates.

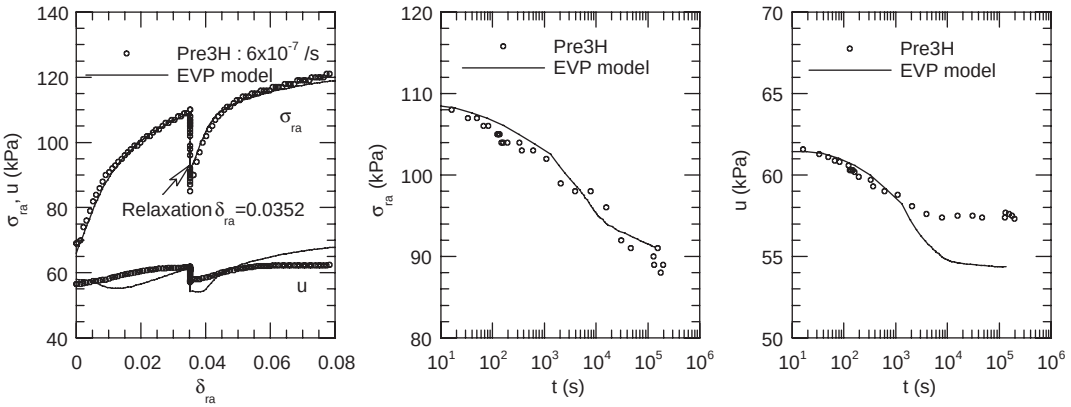

Figure 13. A comparison between experiment and simulation of a pressuremeter strain rate test with a relaxation stage (Pre3H).

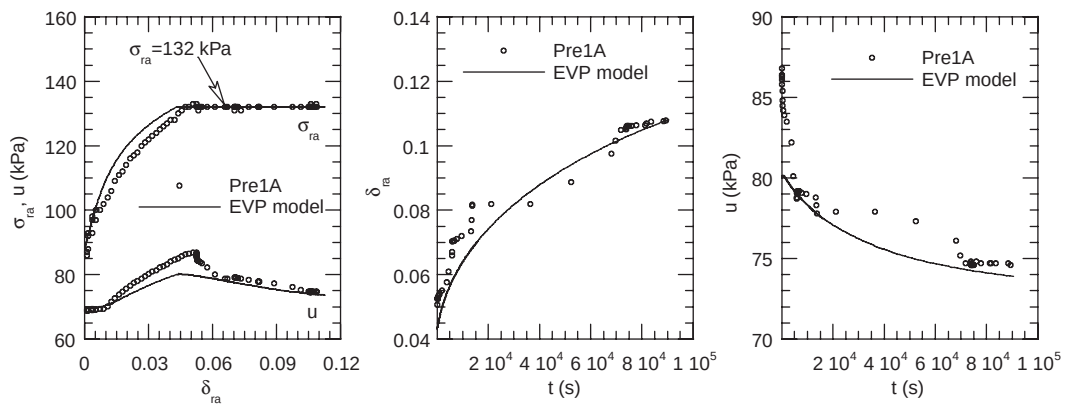

Figure 14. A comparison between experiment and simulation of a pressuremeter creep test (Pre1A).

The identification procedure of the EVP-MCC model parameters was also tested by modelling an undrained triaxial test with three levels of constant strain rates (Tri1B), an undrained triaxial creep test with two levels of deviatoric stress (Tri1F), an oedometer test with different strain rates (Oed1), and an oedometer test under constant loading (Oed2) performed on the same clay sample, as presented in Figures 15 and 16. The value of Young's modulus ($E = 5000\,\text{kPa}$) for the simulation of the triaxial and oedometer tests was taken higher than the one determined from pressuremeter tests due to a different rigidity between vertical and horizontal directions of this anisotropic soil, while the proposed model does not take into account the anisotropy feature of natural soils. Besides this change, all the other parameters were kept at the same values as the ones determined by the identification procedure from pressuremeter tests. We can see in Figures 15 and 16 that a satisfactory agreement was achieved between numerical and experimental results on multiple stages strain rate tests, whereas a global agreement was achieved for creep tests. For these last tests, one should precise that the model cannot reproduce a phase of accelerated creep rate

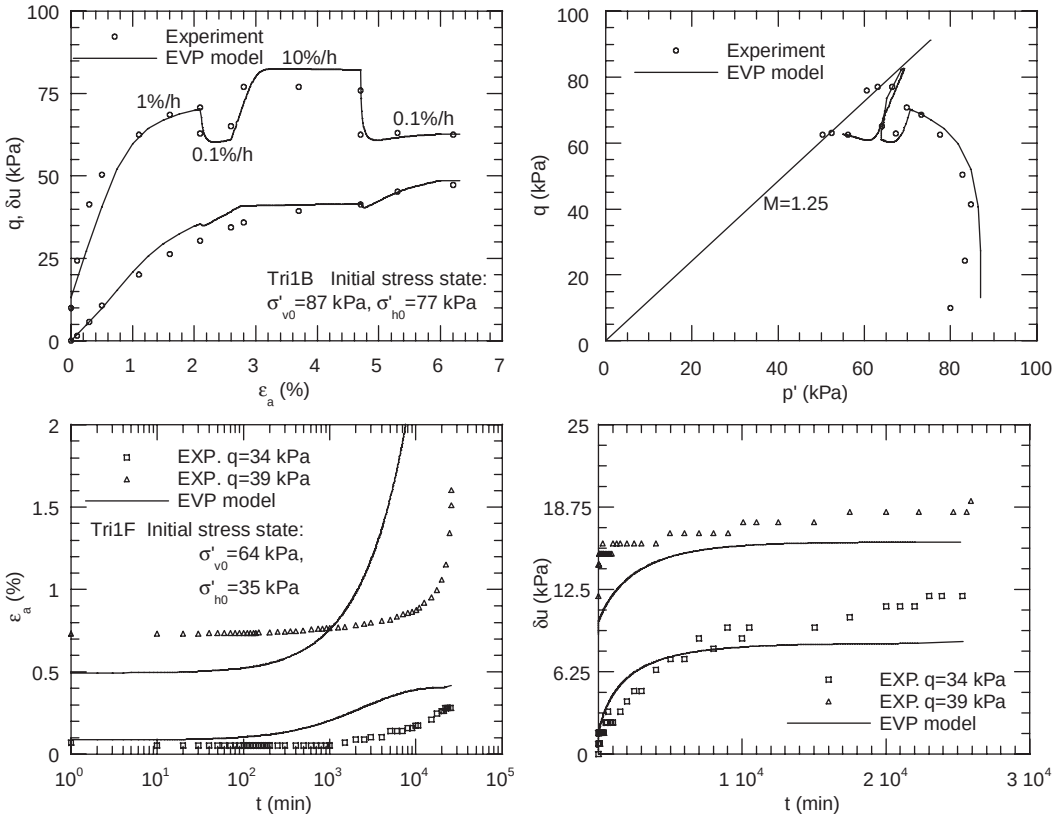

Figure 15. A comparison between experiment and simulation of triaxial tests (Tri1B, Tri1F).

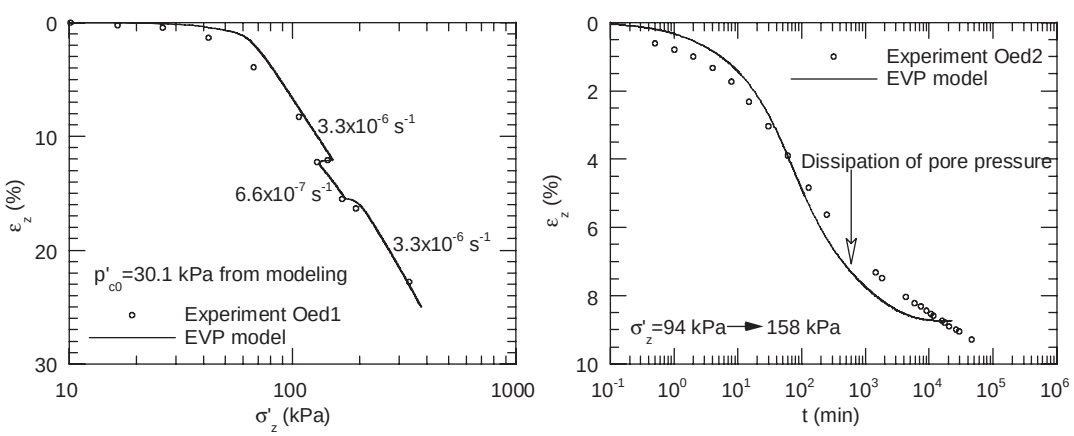

Figure 16. A comparison between experiment and simulation of oedometer tests (Oed1, Oed2).

at failure, called tertiary creep, but predicts instead a constant creep rate when failure is reached. Note that the non-homogeneity of the tested samples and the initial anisotropy feature of natural clay can result in difficulties when several different tests on different specimens are concerned. The identified value of the preconsolidation pressure p'_{c0} is found to agree well with the results obtained from modelling the oedometer test at a constant strain rate.

5. ANALYSIS OF DRAINAGE CONDITIONS

The phenomenon of local consolidation can take place during a pressuremeter test, depending on the strain or stress rate at the cavity wall as well as on the soil permeability. Based on the numerical tests at constant strain rates varying from 6×10^{-2} to $6\times10^{-7}\,s^{-1}$, an analysis of the evolution of the total stress $(\sigma_{ra}-u_0)$ and of the effective stress $(\sigma_{ra}-u)$ at a strain of 8% as a function of $(d\delta_a/dt)/k$ was made using the EVP-MCC parameters determined in Table V. Four different types of behaviour during a pressuremeter test could be observed, as already described by Rangeard *et al.* [8] using the Modified Cam Clay model (Figure 17):

- Fully drained. No excess pore pressure during the pressuremeter test.
- Partially drained type A. The total pressure and the pore pressure are influenced by drainage condition.
- Partially drained type B. The pore pressure is influenced by drainage condition but not the total pressure.
- Fully undrained. The pore pressure evolution remains the same, whereas the total pressure increases with strain rate.

To analyse the drainage conditions for given values of permeability and strain rate, we can transform Figure 17 into the one presented in Figure 18, as described by Rangeard [15]. The points representing each test allow us to determine their drainage conditions. From Figure 18, we observe that Test Pre3B, with the lowest strain rate, is close to fully drained condition. Test Pre3F, with an intermediate strain rate, is in partially drained type A condition. For Tests Pre3A and 3D, both in

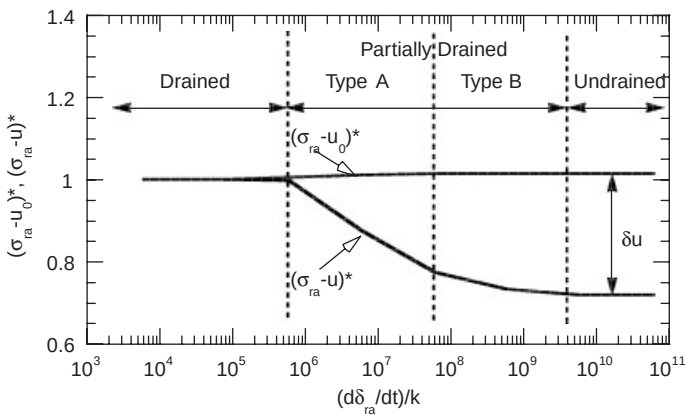

Figure 17. Evolution of $(\sigma_{ra}-u_0)$ and $(\sigma_{ra}-u)$ as a function of $(d\delta_a/dt)/k$.

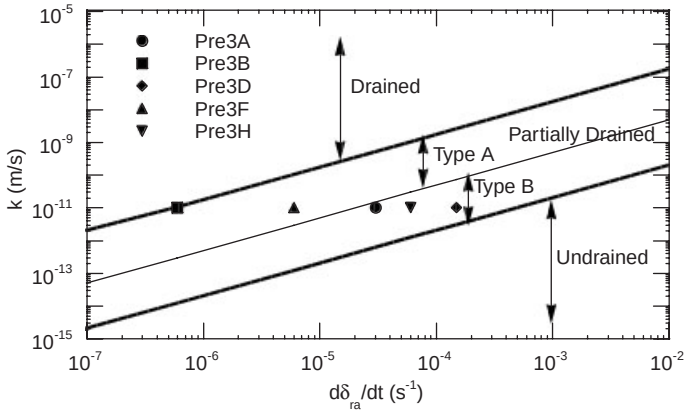

Figure 18. Drainage conditions as a function of strain rate and permeability.

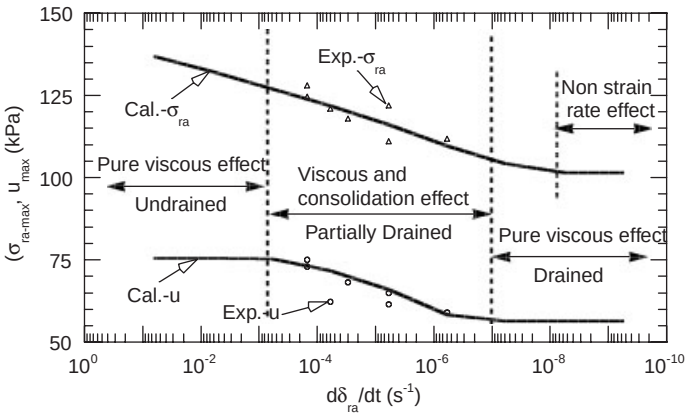

Figure 19. Strain rate effects during pressuremeter tests on Saint-Herblain clay.

partially drained type B condition, the difference in total pressure for different strain rates is due to the viscous behaviour of the soil skeleton.

The strain rate effects in pressuremeter tests on Saint-Herblain clay were studied based on the determined soil parameters. The total stress and pore pressure at the cavity wall, at a strain of 8%, as a function of the logarithm of the strain rate are presented in Figure 19. The prediction for the strain rate varying from 1.5×10^{-4} to $6\times10^{-7}\,s^{-1}$ agrees with experimental results. The total stress and the pore pressure increase with the strain rate due to the viscous properties as well as due to the different drainage conditions. As for other strain rates, we note that:

- For a strain rate higher than $6\times10^{-4}\,s^{-1}$, the consolidation effect is erased due to fully undrained condition. The total stress or the effective stress increases linearly with the logarithm of the strain rate due to the viscous properties only, as described by Vaid and Campanella [18] for undrained triaxial tests.
- For a strain rate smaller than $6\times10^{-8}\,s^{-1}$, no pore pressure is generated due to fully drained condition. The total stress or the effective stress decreases down to a constant value with the

Table VI. Values of EVP-MCC model and hydraulic parameters for Burswood clay.

Sites	E (kPa)	υ	β^*	M	p'_{c0} (kPa)	N	μ ($s^{-1}kPa^{-1}$)	k (m/s)
Burswood	4000	0.3	0.07	1.45	38	12	2×10^{-7}	3.3×10^{-9}

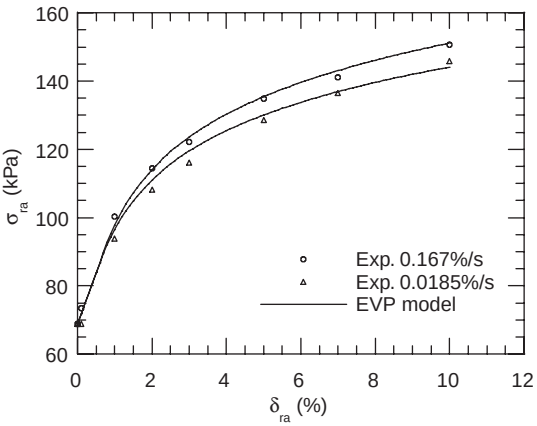

Figure 20. A comparison between predicted and experimental results for SBP tests on Burswood clay.

decrease in the strain rate only because of the viscous properties. This effect decreases for low strain rates, and therefore strain rates smaller than $1\times10^{-8}\,s^{-1}$ on Saint-Herblain clay can erase either viscous or consolidation effect.

6. APPLICATION TO *IN SITU* PRESSUREMETER TESTS

SBP tests were performed in the Burswood Peninsula site at a depth of 5.25 m by Lee and Fahey [19]. The expansion phase was conducted at two different rates to around 10% cavity strain: 0.167 and 0.0185%/s. The parameters from oedometer and triaxial tests by Lee and Fahey [19] with viscosity parameters determined by the proposed procedure of parameter identification are summarized in Table VI.

Figure 20 compares the predicted and measured results for SBP tests in terms of total pressure at the cavity wall *versus* cavity strain. The proposed methodology by inverse analysis is found efficient for identifying soil parameters from *in situ* testing.

7. CONCLUSION

The possibility of determining viscous properties from *in situ* testing has been discussed. An inverse analysis method for identifying soil parameters from constant strain rate pressuremeter tests has been proposed. This method of identification was employed to determine the parameters of an elasto-viscoplastic model, the EVP-MCC model, as well as the soil permeability. The procedure was applied to a soft clay, the Saint-Herblain clay. The procedure was then verified by comparing the optimized values of the soil parameters and the values of the same parameters obtained from

laboratory test results. Additional validation was also performed by using the identified parameters to simulate other tests on the same samples, such as pressuremeter tests at a constant strain rate and with a relaxation or a creep stage, triaxial and oedometer tests. The values of the parameters obtained from pressuremeter tests agreed with those obtained from triaxial and oedometer tests. This showed that the soil parameters could be adequately identified by pressuremeter tests with three different strain rates.

A drainage condition analysis has then been performed by observing the evolution of the total and the effective pressure at the cavity wall as a function of the strain rate and the permeability. Four different types of drainage conditions have been defined by the value of the ratio between strain rate and permeability. The drainage conditions of the pressuremeter tests performed on Saint-Herblain clay were then determined. The results show that the strain rate effects are due to both the viscous properties and the consolidation condition during a pressuremeter test in field.

All the numerical simulations have shown that the proposed methodology is efficient to be used for identifying soil parameters, and the EVP-MCC model could adequately describe the time-dependent behaviour of soft soils under different monotonic loading conditions. Further validation for the parameter identification is needed, such as the prediction of the behaviour of infrastructures built on soft clay by using the recorded deformations during the construction.

NOTATIONS

$C_{\alpha e}$	coefficient of secondary compression
e_0	void ratio
f_s	static yield function
f_d	dynamic yield function
p'	mean effective stress
p_c^s	static hardening parameter
p_c^d	dynamic hardening parameter
$p'_{\mathrm{c}0}$	preconsolidation pressure
q_f	undrained shear strength
s'_{ij}	effective deviatoric stress tensor
E	Young's modulus
G	elastic shear modulus
K	elastic bulk modulus
M	slope of critical state line
β^*	compressibility index
δ_{ij}	Kronecker's delta
ε_{ij}	strain tensor
$\varepsilon_{ij}^{\mathrm{vp}}$	viscoplastic strain tensor
κ	swelling index
λ	compression index
ρ_{a0}	strain rate parameter
σ'_{ij}	effective stress tensor
υ	Poisson's ratio
Δd	vector of nodal displacements
Δu_w	incremental pore-water pressure vector

$[B]$ strain–displacement transformation matrix
$[D_e]$ elastic matrix
ΔF vector of nodal loads
ΔF_b incremental body force vector
ΔT incremental surface force vector

ACKNOWLEDGEMENTS

The research reported in this paper is funded by a grant from 'Conseil Regional des Pays de la Loire'. The authors thank Dr Christophe Dano and Dr Yvon Riou, associate professors at Research Institute in Civil and Mechanical Engineering of Ecole Centrale de Nantes, and professor Hong-Wei Huang in Tongji University for their support.

REFERENCES

1. Menard L. Pressiometre. Brevet Francais d'invention. No.1.117.983, 1955.
2. Zentar R, Hicher PY, Moulin G. Identification of soil parameters by inverse analysis. *Computers and Geotechnics* 2001; **28**(2):129–144.
3. Calvello M, Finno RJ. Selecting parameters to optimize in model calibration by inverse analysis. *Computers and Geotechnics* 2004; **31**(5):411–425.
4. Anderson WF, Pyrah IC, Ali FH. Rate effects in pressuremeter tests in clays. *Journal of Geotechnical Engineering* (ASCE) 1987; **113**(11):1344–1358.
5. Bahar R, Cambou B, Fry JJ. Forecast of creep settlements of heavy structures using pressuremeter tests. *Computers and Geotechnics* 1995; **17**(4):507–521.
6. Pye CN. Influence of constitutive models on self-boring pressuremeter interpretation in clay. *Canadian Geotechnical Journal* 1995; **32**(3):420–427.
7. Hicher PY, Michali A. Identifying soil parameters by means of laboratory and in situ testing. *Computers and Geotechnics* 1996; **19**(2):153–170.
8. Rangeard D, Hicher PY, Zentar R. Determining soil permeability from pressuremeter tests. *International Journal for Numerical and Analytical Methods in Geomechanics* 2003; **27**(1):1–24.
9. Yin ZY, Hicher PY, Riou Y, Huang HW. An elasto-viscoplastic model for soft clay. *Soil and Rock Behavior and Modeling—Proceedings of the Geoshanghai Conference*, vol. 150, Shanghai, Geotechnical Special Publication, 2006; 312–319.
10. Perzyna P. The constitutive equations for work-hardening and rate sensitive plastic materials. *Proceedings of Vibration Problems*, vol. 3, Warsaw, 1963; 281–290.
11. Perzyna P. Fundamental problems in viscoplasticity. *Advances in Applied Mechanics* 1966; **9**:243–377.
12. Oka F, Adachi T, Okano Y. Two-dimensional consolidation analysis using an elasto viscoplastic constitutive equation. *International Journal for Numerical and Analytical Methods in Geomechanics* 1986; **10**(1):1–16.
13. Hinchberger SD, Rowe RK. Modelling the rate-sensitive characteristics of the Gloucester foundation soil. *Canadian Geotechnical Journal* 1998; **35**(5):769–789.
14. Britto AM, Gunn MJ. *Critical State Soil Mechanics via Finite Elements*. Ellis Horwood: Chichester, England, 1987.
15. Rangeard D. Identification des caractéristiques hydro-mécaniques d'une argile par analyse inverse des essais pressiométriques. Thèse de l'Ecole Centrale de Nantes et l'Université de Nantes, 2002.
16. Zentar R. Analyse inverse des essais pressiometrique, application a l'argile de Saint-Herblain. Thèse de l'Ecole Centrale de Nantes et l'Université de Nantes, 1999.
17. Yin ZY. Modelisation viscoplastique des argiles naturelles et application au calcul de remblais sur sols compressibles. Thèse de l'Ecole Centrale de Nantes et l'Université de Nantes, 2006.
18. Vaid YP, Campanella RG. Time-dependent behavior of undisturbed clay. *Journal of the Geotechnical Engineering* (ASCE) 1977; **103**(7):693–709.
19. Lee Goh A, Fahey M. Application of a 1-dimensional cavity expansion model to pressuremeter and piezocone tests in clay. *Proceeding of the Seventh International Conference on Computer Methods and Advances in Geomechanics*, Cairns, 1991; 255–260.